Preprints.org

Article

Evaluation of Sentinel-3 SYN VGT Products in Comparison to the SPOT/VEGETATION and PROBA-V Archives

Carolien Toté [*] , Else Swinnen , Claire Henocq

Article

Evaluation of Sentinel-3 SYN VGT Products in Comparison to the SPOT/VEGETATION and PROBA-V archives

Carolien Toté [1],*, Else Swinnen [1] and Claire Henocq [2]

[1]   Flemish Institute for Technological Research (VITO), Boeretang 200, B-3200 Mol, Belgium; else.swinnen@vito.be (E.S.)

[2]   ACRI-ST, 260 Route du Pin Montard, BP 234, 06904 Sophia-Antipolis, France; claire.henocq@acri-st.fr

*   Correspondence: carolien.tote@vito.be; Tel.: +32-14-336844

Abstract: Sentinel-3 synergy (SYN) VEGETATION (VGT) products were designed to provide continuity to SPOT/VEGETATION (SPOT VGT). In past years, important changes have been implemented in the SYN VGT processing baseline. Since the PROBA-V mission acted as a gap filler between SPOT VGT and Sentinel-3, and in principle a continuous series of data products from the combined data archives of SPOT VGT (1998 – 2014), PROBA-V (2013-2020) and Sentinel-3 SYN VGT (from 2018 onwards) is available to users, consistency of Sentinel-3 SYN VGT with both the latest SPOT VGT (VGT-C3) and PROBA-V (PV-C2) archives is highly relevant. Spatio-temporal intercomparison of the combined time series of VGT-C3, PV-C2 and Sentinel-3 SYN VGT 10-day NDVI composite products with an external reference from LSA-SAF, and the intercomparison of Sentinel-3 SYN V10 products with a climatology of VGT-C3 resp. PV-C2 for 3 distinct periods with different levels of product quality have shown that the subsequent processing baseline updates have resulted in better quality products. It is therefore essential to reprocess the entire Sentinel-3 SYN VGT archive: a uniform data record of standard SPOT VGT, PROBA-V and Sentinel-3 SYN VGT products, spanning over 25 years, would provide valuable input for a wide range of applications.

Keywords: Sentinel-3; SPOT/VEGETATION; PROBA-V; surface reflectance; NDVI; long term data record; consistency

1. Introduction

Sentinel-3A was launched on 16 February 2016 and accompanied by Sentinel-3B on 25 April 2018, with onboard multiple sensing instruments focusing on Earth observation to support Copernicus ocean, land, atmosphere, emergency, security and cryosphere applications. Co-located observations of two of these instruments – the Ocean and Land Colour Instrument (OLCI) and the Sea and Land Surface Temperature Radiometer (SLSTR) – are used as synergistic input to the so-called 'synergy' (SYN) processing chain [1].

The Sentinel-3 SYN processing chain combines observations in the visible and near-infrared (VNIR) and short-wave infrared (SWIR) channels to provide several higher level products. One particular series of output products of the SYN processing chain are the SYN VEGETATION (SYN VGT) products, that are designed to provide surface reflectance products similar to those obtained from the VEGETATION1 and VEGETATION2 (VGT) instruments onboard SPOT4 (launched 24 March 1998) and SPOT5 (launched 4 May 2002), respectively, to meet Copernicus – previously known as Global Monitoring for Environment and Security (GMES) – user needs [2].

SPOT5 was however decommissioned early 2015, i.e. before the launch of the first Sentinel-3 satellite. From 2013 to 2020, PROBA-V (Project for On-Board Autonomy – Vegetation), launched 7 May 2013, provided data continuity to the SPOT VGT payloads and acted as a gap-filler to the Sentinel-3 mission [3]. The PROBA-V mission was designed and products had been defined to closely match SPOT VGT products [4], and also after the latest reprocessing campaigns, both the SPOT VGT Collection 3 and PROBA-V Collection 2 archives were shown to be highly consistent [5,6].

Similar to the standard products of SPOT VGT and PROBA-V, Sentinel-3 SYN VGT products provide complete Earth coverage every 1 to 2 days in 4 spectral bands (BLUE, with central wavelength 450 nm; RED, 645 nm; NIR, 835 nm; and SWIR, 1665 nm), projected on a regular 1 km "Plate carrée" grid [1]. Output products include (i) top-of-atmosphere (TOA) reflectance (VGP); (ii) 1-day synthesis surface reflectance and Normalized Difference Vegetation Index (NDVI) (VG1); and (iii) 10-day synthesis surface reflectance and NDVI (V10).

In principle, user thus have access to a continuous series of data products from the combined data archives of SPOT VGT (1998 – 2014), PROBA-V (2013-2020) and Sentinel-3 SYN VGT (from 2018 onwards). There are however several aspects related to the satellite/sensor and processing definitions that to a greater or lesser extent impact the consistency between these product series, such as differences in the acquisition scheme, sensor design, spectral response, atmospheric correction and sensor calibration. Another crucial aspect is that since the release of the first Sentinel-3 SYN VGT products in October 2018, several important changes in the SYN VGT processing baseline have been implemented, thereby gradually improving the quality of the SYN VGT products. However, up to now no reprocessing of the SYN VGT archive has taken place. The archive of SYN VGT products is therefore intrinsically inconsistent and consequently different consistency levels with SPOT VGT and PROBA-V will be reached throughout the years.

The goal of this paper is to evaluate how these consecutive improvements in the SYN processing have (positively) affected the level of consistency of Sentinel-3 SYN VGT V10 products with SPOT VGT Collection 3 and PROBA-V Collection 2 products, and what level of consistency is reached in the SYN VGT products that are currently made available shortly after new Sentinel-3 OLCI and SLSTR acquisitions. Furthermore, we aim to inform users about the quality concerns present in the current SYN VGT dataset, particularly when these products are used alongside the SPOT VGT and PROBA-V product archives.

To reach these goals, in first instance we compared the combined time series of 10-day NDVI synthesis products from SPOT VGT, PROBA-V and Sentinel-3 SYN VGT with an external NDVI time series derived from the Advanced Very High Resolution Radiometer (AVHRR) onboard the METOP satellites. Secondly, Sentinel-3 SYN VGT V10 products for 3 distinct periods with different levels of product quality were compared to 5-year climatology products derived from SPOT VGT and PROBA-V, respectively.

2. Materials and Methods

2.1. Data

2.1.1. Sentinel-3 SYN VGT V10

Sentinel-3 SYN VGT products and processing steps are described by [1]. In summary, the SYN VGT processing module consists of: (i) the Level-1 module dedicated to the co-registration of OLCI and SLSTR acquisitions and the production of internal SYN Level-1 products, (ii) the SYN Level-2 module dedicated to aerosol retrieval and atmospheric correction, and (iii) the SYN VGT module that performs spectral mapping to simulate the SPOT VGT or PROBA-V spectral bands, projection and compositing to generate simulated VGP, VG1 and V10 products [7]. In this study, we focus on the V10 products, i.e. 10-daily maximum NDVI value composites of surface reflectance measurements and the NDVI.

As highlighted above, important updates, improvements and bug fixes have been implemented to the SYN VGT processing lines since the first release of SYN VGT products in 2018 (exact dates and processing baseline documents are available on https://sentiwiki.copernicus.eu/web/synergy-processing). The most impactful changes are listed here and schematized in Figure 1:

- September 2019: Correction in the product gridding to correct for a 0.5 pixel displacement in latitude and longitude direction. Measurements are provided on the same regular latitude-longitude grid as previous SPOT VGT and 1 km PROBA-V products, with an equatorial sampling distance of approximately 1 km (1°/112).

- June 2020: Alignment of the temporal compositing scheme of 1-day and 10-day synthesis products with previous SPOT VGT and PROBA-V products. Per month, three V10 products are provided, based on observations in days 1-10, 11-20 and 21-end of the month, respectively.
- June 2021: Correction in the definition of VG1 and V10 NDVI to be based on surface reflectance in the RED and NIR bands. Until May 2021, the NDVI products were erroneously based on top-of-atmosphere (TOA) reflectances.
- August/September 2022: Improved handling of saturated values.
- July 2023: The last important update includes two aspects: (i) correction in the spectral band mapping procedure and (ii) S3A/OLCI and SLSTR calibration adjustments. The first aspect includes the change to the use of PROBA-V spectral response functions (instead of SPOT4/VGT1) in the spectral band mapping procedure. Although differences between the spectral responses between SPOT VGT and PROBA-V are rather small [3], this change has slight impact on the retrievals in the RED and SWIR bands. Much larger impact is induced by the implementation of important bug fixes, including correct exclusion of atmospheric absorption bands and correct handling of wavelength units. The second aspect includes application of a 2% calibration bias correction on S3A OLCI, as evidenced through the tandem phase study [8], and application of the Sentinel-3 SLSTR vicarious calibration adjustments [9].

For the statistical evaluation of the consistency between SYN VGT products and the SPOT VGT and PROBA-V product archives, 3 periods of 12 months were selected in between these processing baseline updates (Figure 1):

- Period 1 (P1): June 2020 – May 2021
- Period 2 (P2): August 2021 – July 2022
- Period 3 (P3): August 2023 – July 2024

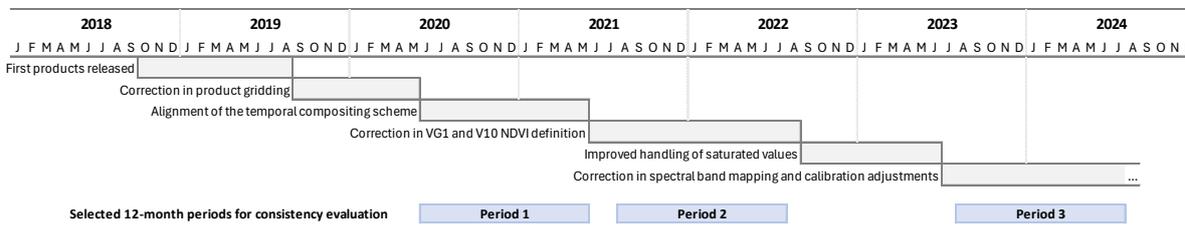Sentinel-3 SYN VGT products are made available through the Copernicus Data Space Ecosystem (https://dataspace.copernicus.eu/).

Figure 1. Timeline of Sentinel-3 SYN VGT product updates. Three 12-month periods are identified for further analysis.

2.1.2. SPOT VGT Collection 3 Level 3 S10-TOC

After the end of the SPOT VGT mission in May/2024, the complete archive was reprocessed, resulting in the Collection 3 archive (VGT-C3) [10]. The VGT-C3 Level-3 10-daily top-of-canopy (TOC) synthesis products (S10-TOC) containing surface reflectance and NDVI from 2009 till June/2014 were used in this study. For more details on the processing of SPOT VGT data, we refer to the SPOT VGT Products User Manual [11].

From 2009 onwards, SPOT5 experienced orbital drift, causing the satellite overpass time to gradually shift over time. This evolution causes small but systematic changes in illumination conditions and related Bidirectional Reflectance Distribution Function (BRDF) effects; e.g. NDVI tends to increase with higher solar zenith angles [12–14].

VGT-C3 data products are available through the Terrascope platform (https://www.terrascope.be).

2.1.3. PROBA-V Collection 2 Level 3 S10-TOC

Designed as a successor for the SPOT VGT, the PROBA-V mission provides continuity products to SPOT VGT, although also products at higher spatial resolution (300 m and 100 m) are disseminated.

Detailed descriptions of the PROBA-V mission and processing chains are provided by [4] and [15]. Also the PROBA-V archive was reprocessed after the end of its operational lifetime, aiming at improving the time series and harmonizing its content. The resulting Collection 2 (PV-C2) was released in 2023 [16]. In this study, we use PV-C2 Level-3 S10-TOC surface reflectance and NDVI for the period January 2014 – June 2020.

It should be noted that at the time of the switch between SPOT VGT and PROBA-V, there was an important difference in the equator local overpass times between SPOT5 and PROBA-V. Since PROBA-V had no onboard propulsion, the satellite experienced a constantly varying overpass time.

PV-C2 data products are available through the Terrascope platform (https://www.terrascope.be).

2.1.4. LSA-SAF METOP/AVHRR ENDVI10 Version 2

The EUropean organisation for the exploitation of METeorological SATellites (EUMETSAT) Polar System (EPS) consists of a series of polar orbiting meteorological satellites, known as METOP. The AVHRR-instruments onboard METOP are used to generate 10-daily Enhanced NDVI (ENDVI10) by the Land Surface Analysis Satellite Application Facility (LSA-SAF). The ENDVI10 version 2 is processed in a similar way to the S10-TOC of PROBA-V, with the same water vapor and ozone inputs, and a similar atmospheric correction and compositing method [17]. There are however differences in spectral response, calibration, cloud detection, and overpass time stability. Global ENDVI10 version 2 products derived from METOP-A (launched 19 October 2006) for the period January 2009 – April 2013, and METOP-B (launched 17 September 2012) for the period May 2013 – July 2024 are used in the evaluation as an external reference.

2.3. Methods

2.3.1. Sampling

A systematic spatial subsample is taken from each global product by considering one pixel of every 20 in both latitude and longitude direction. This (arbitrary) subsample is representative for the global patterns of vegetation and considerably reduces processing time, while retaining the original resolution.

Only pixels that are not identified as cloud, cloud shadow or snow in the respective product status maps are considered for the analyses. For PV-C2 data, also the aerosol optical thickness (AOT) mask is applied, and observations affected by high AOT (AOT ≥ 0.8) are discarded [16].

In order to evaluate gradual changes in SYN VGT data quality, temporal sampling of SYN VGT V10 products includes the delineation of three 12-month periods P1, P2 and P3 (see above).

2.3.2. Long Term Statistics

Long term statistics (LTS) are retrieved from the extracted VGT-C3 and PV-C2 spatial subsamples by calculating an average value for each 10-day period in the year and for each sample. Both for VGT-C3 and PV-C2 a 5-year period is considered for LTS calculation: 2009-2013 for VGT-C3, 2014-2018 for PV-C2, respectively. The resulting climatology for each product series is a measure of the average status of the surface for the respective LTS periods and is used as the reference in statistical intercomparison.

2.3.3. Geometric Mean Regression and Coefficient of Determination (R^2)

The geometric mean (GM) regression model is used to identify the relationship between two datasets of remote sensing measurements. Because both data sets (X: reference, Y: product under evaluation) in this case are subject to noise, it is appropriate to use an orthogonal (model II) regression. The GM regression model minimizes the sum of the products of the vertical and horizontal distances (i.e. errors on both X and Y). By applying an eigen decomposition to the covariance metrics of X and Y, two eigenvectors are obtained that describe the principal axes of the point cloud [18].

The coefficient of determination (R²) indicates agreement or covariation between two data sets with respect to the linear regression model. It summarizes the total data variation explained by this linear regression model – higher R² values indicate higher covariation.

2.3.4. APU Metrics

The deviations between two data sets are evaluated through assessment of the Accuracy, Precision and Uncertainty (*APU*) metrics [19]. The Accuracy (*A*) or mean bias measures the average actual difference between two data sets X and Y:

$$A = \frac{1}{n}\sum_{i=1}^{n}(X_i - Y_i) = \bar{X} - \bar{Y} \tag{1}$$

As such, *A* retains the sign of the difference between the data sets and is a measure for systematic bias. The Precision (*P*) or repeatability represents the dispersion of product retrievals around their expected value and is estimated by the standard deviation of the bias between retrieved satellite products:

$$P = \sqrt{\frac{1}{n-1}\sum_{i=1}^{n}(X_i - Y_i - A)^2} \tag{2}$$

Finally, the Uncertainty (*U*) is defined as the overall difference, including random and systematic differences, and is measured through the root mean squared difference:

$$U = \sqrt{\frac{1}{n}\sum_{i=1}^{n}(X_i - Y_i)^2} \tag{3}$$

High *APU* values reflect discrepancies between two compared data sets whereas low values indicate high consistency [20].

2.3.5. Hovmöller Diagrams

In order to perform a combined assessment of the spatial and temporal variability of the *APU* metrics of the intercomparison between the combined time series of 10-day NDVI synthesis products from VGT-C3, PV-C2 and SYN V10 on one hand with the stable time series of ENDVI10 on the other hand, Hovmöller diagrams are made. The metrics are derived on the global subsample for each time step (10-day period) and for each secondary spatial subset, defined as latitude bands of 12°. The resulting time-latitude Hovmöller diagrams allow summarizing the space-time features of the time series evaluation, thereby depicting the temporal evolution of the spatial agreement [21].

3. Results and Discussion

3.1. Spatio-Temporal Intercomparison with LSA-SAF ENDVI10

As the ultimate goal of the Sentinel-3 SYN VGT products is to provide continuity to the SPOT VGT and PROBA-V product archives, we focus first on the spatio-temporal intercomparison of the combined series with an external dataset. The Hovmöller plots of the intercomparison between LSA-SAF ENDVI and the combined series of 10-day NDVI composites from VGT-C3 (2009-2013), PV-C2 (2014-June 2020) and S3A SYN VGT (July 2020-July 2024) are illustrated in Figure 2. These allow to get a broad overview of the temporal stability of the Sentinel-3 SYN V10 NDVI product in relation to the SPOT VGT and PROBA-V archives. The results for S3B SYN V10 are very similar and not shown.

Whereas higher values for *P* and *U* are observed around the equator and up to 20° S in the Southern hemisphere summer period, these (mostly densely vegetated) areas show in general a lower *A*: average bias between both time series is lower, but with higher dispersion. This could be related to a larger influence of atmospheric effects in Tropical areas and more cloud contamination that is still present in the maximum NDVI-value composites [22].

The three 12-month periods that are used to evaluate the Sentinel-3 SYN V10 products consistency with the SPOT VGT and PROBA-V data archives are delineated in Figure 2. An important discontinuity in A and U is observed at the switch from PROBA-V to S3A (July 2020). This is caused by the fact that before June 2021 (i.e. in P1), Sentinel-3 SYN V10 was (incorrectly) based on TOA reflectances. After the correction, in P2 A stabilizes, but at a rather high level. The corrections implemented in July 2023 result in A closer to zero in P3.

Towards the end of both the SPOT VGT (2013) and PROBA-V (June 2020) periods, a deviation of A is visible. Orbital drift of both instruments (see above) lead to gradually earlier overpass times resulting in increasing solar zenith angles. Although the effects of the orbital drift have been reported to be mitigated to some extent in the NDVI [14,23], the effect is not negligible, and can only be mitigated through anisotropy correction based on the BRDF [24,25].
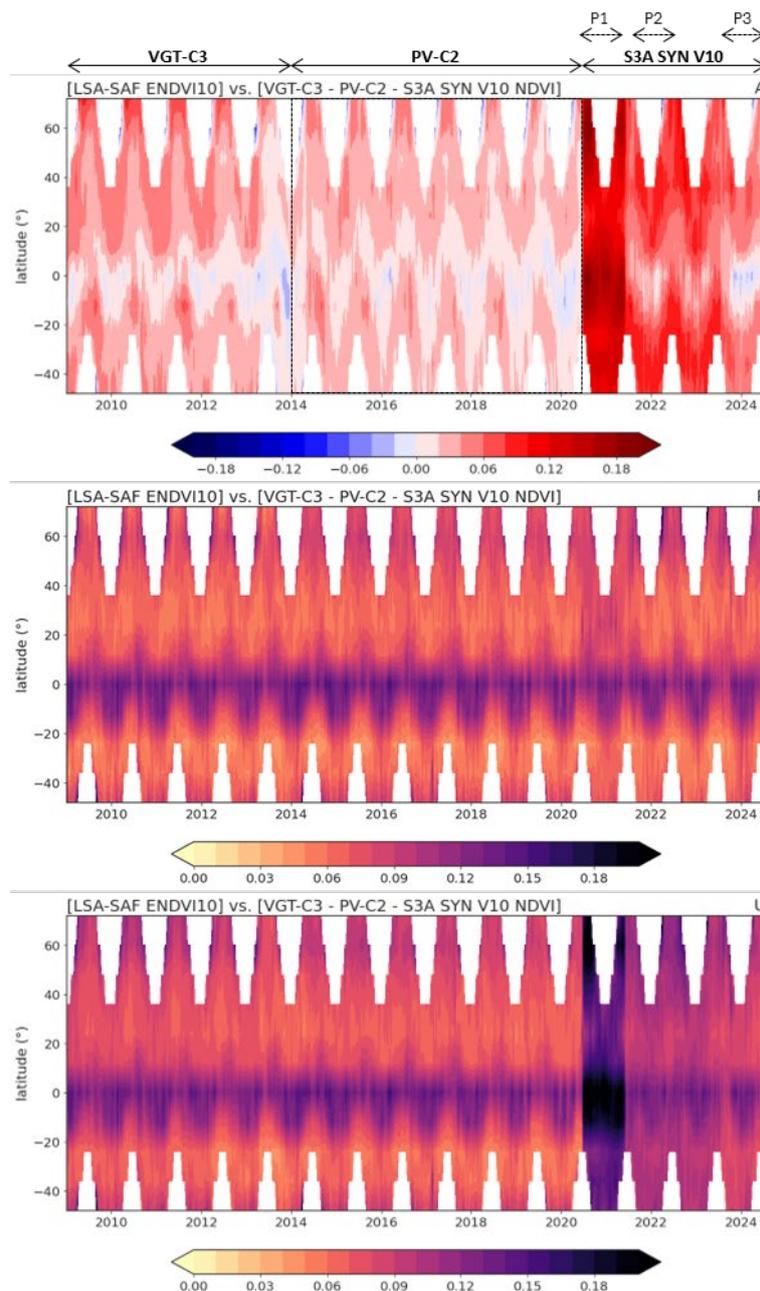

Figure 2. Hovmöller plots of the *APU* metrics between LSA-SAF ENDVI and the combined NDVI series of VGT-C3 (2009-2013), PV-C2 (2014-June 2020) and S3A SYN V10 (July 2020-July2024). The metrics are derived on 12° latitude band samples for each 10-day period.

3.2. Intercomparison with VGT-C3 and PV-C2 LTS for P1, P2 and P3

In order to evaluate the evolution of the consistency between Sentinel-3 SYN V10 and the SPOT VGT and PROBA-V data archives, Figure 3 and Figure 4 show the results of the statistical consistency analysis between VGT-C3 LTS resp. PV-C2 LTS and S3A SYN V10, for P1, P2 and P3 and for the NDVI and 4 spectral bands. The results for S3B are very similar and are not displayed.

The large scatter in the scatter density plots overall (leading to high values for *P*) is partly related to the fact that two different periods are compared: the 5-year period on which the respective LTS are based, versus the 12-month periods in the more recent SYN V10 products archive. Land cover transitions, e.g. vegetation loss, urban expansion, reforestation or agricultural expansion, will have taken place on the surface in a minority of the pixels sampled. Also natural fluctuations in vegetation development occur, plus human-induced variations, such as e.g. crop rotation. In addition, and more importantly, the satellite observations are influenced by angular and atmospheric effects, although these effects are attenuated to some extent through the maximum NDVI-value composite algorithm [26] that is used to generate the 10-daily composite products. Both SPOT VGT and PROBA-V have a very wide swath coverage, with swath widths above 2200 km, whereas both OLCI and SLSTR have a more narrow swath (around 1400 km). The OLCI swath is not centred at nadir but tilted 12.6° westward to minimize the impact of sun glint contamination [2]. In addition, whereas Sentinel-3 flies in a sun-synchronous orbit with descending node equatorial crossing at 10h mean local time, both SPOT VGT and PROBA-V were experiencing orbital drift (see above). Different sampling in both viewing and illumination angles contributes to unsystematic differences observed in the comparison. Secondly, incomplete cloud and cloud shadow masking can influence the intercomparison, especially in areas with persistent cloud cover where the probability of not having a clear sky observations in the 10-day compositing period is higher. In this respect, it is to be noted that currently no cloud shadow masking is done in Sentinel-3 SYN VGT products. Finally, differences in atmospheric correction lead to unsystematic differences in the TOC reflectances and NDVI. One aspect is the estimation of aerosol optical thickness (AOT). For VGT-C3 atmospheric correction, AOT is estimated from the BLUE band and the NDVI through an optimization process [27]. PV-C2 uses an external AOT dataset, namely the MERRA-2 (Modern-Era Retrospective analysis for Research and Applications, version 2) as input to the atmospheric correction [28]. In the Sentinel-3 SYN Level-2 processing, AOT is retrieved using collocated OLCI and SLSTR TOA radiances based on methods developed for the predecessors of both sensors [29], and previous studies have shown that this AOT tends to be overestimated [30].

Apart from the large scatter, discussed above, overall high linear correlations are found between the VGT-C3 resp. PV-C2 LTS and the SYN V10 products, with R² values around or well above 0.7. The largest discrepancies are found for the NDVI in P1, with GMR slope well below 1, and for the SWIR band in P1 and P2, with GMR intercepts well below 0. Figure 5 shows the gradual improvements in *APU* statistics from P1 over P2 to P3. The largest improvement for the NDVI, leading to a drop in *A* from 0.1 to 0.05 (in comparison to SPOT VGT) and 0.04 (in comparison to PROBA-V), is related to the correction in the definition of the product in June 2021: in P1, the product was incorrectly based on TOA reflectances. Finally, corrections and adaptations in the spectral band mapping and calibration, applied in July 2023 (P3), result in *A* around 0.02 and 0.01 in comparison to SPOT VGT and PROBA-V, respectively. This effect is obtained by small improvements in the consistency for the RED band. The largest effects of the changes applied in July 2023 are visible in the SWIR band, where *A* drops from around 0.09 in P1 and P2 to values around -0.02 in P3.

The overview of the *APU* statistics in Figure 5 also shows that there is very little difference between the results based on Sentinel-3A and Sentinel-3B SYN V10 products. The application of the OLCI-A calibration adjustments (implemented between P2 and P3) seem to have only minor impacts. Values for *P* remain roughly constant over the three periods, because the reasons for high scatter in the comparison (see above) have not been influenced by the subsequent processing baseline updates.
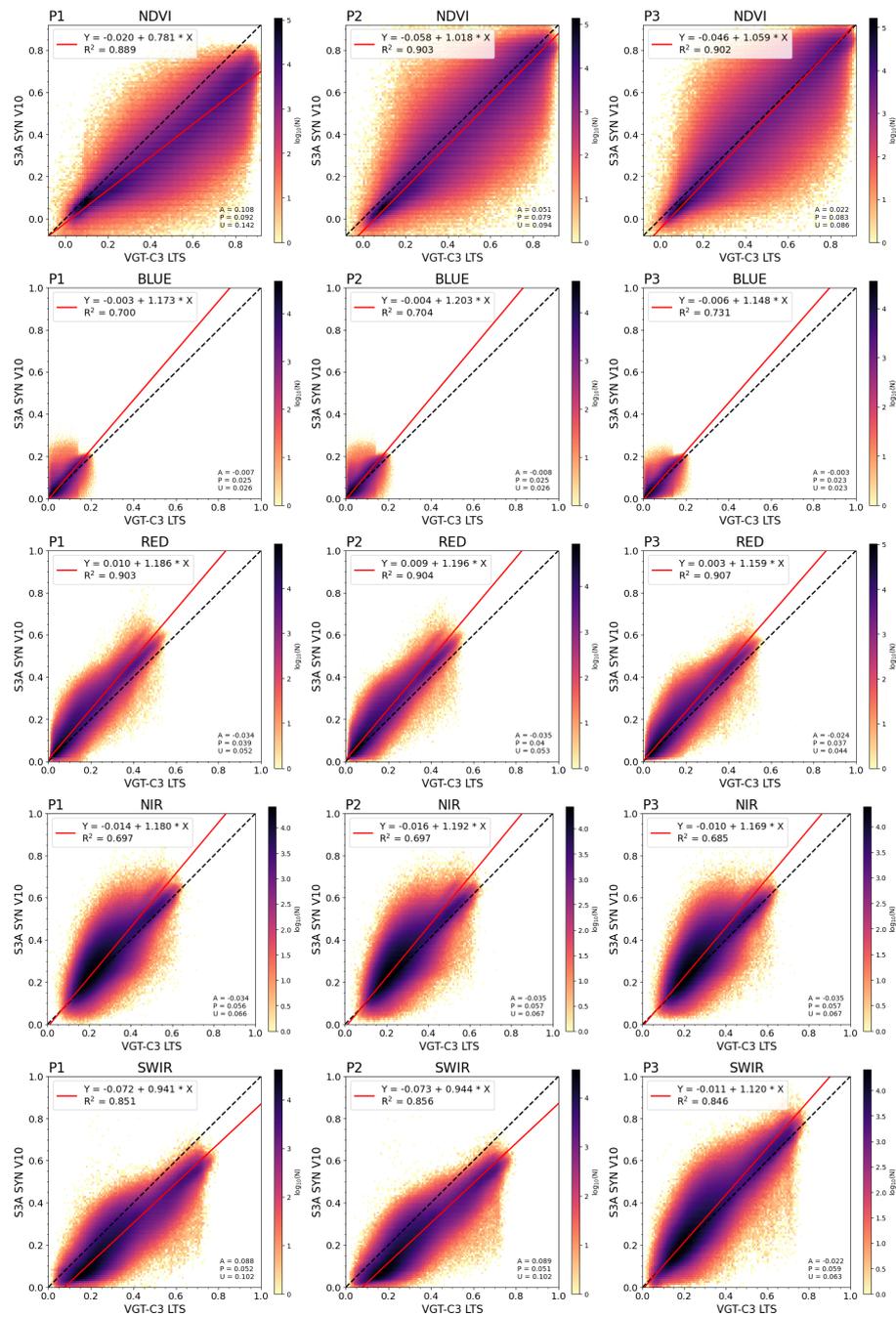
Figure 3. Scatter density plots and GM regression between VGT-C3 LTS (X) and S3A SYN V10 (Y) for P1 (left), P2 (middle) and P3 (right). From top to bottom: NDVI, BLUE, RED, NIR and SWIR.
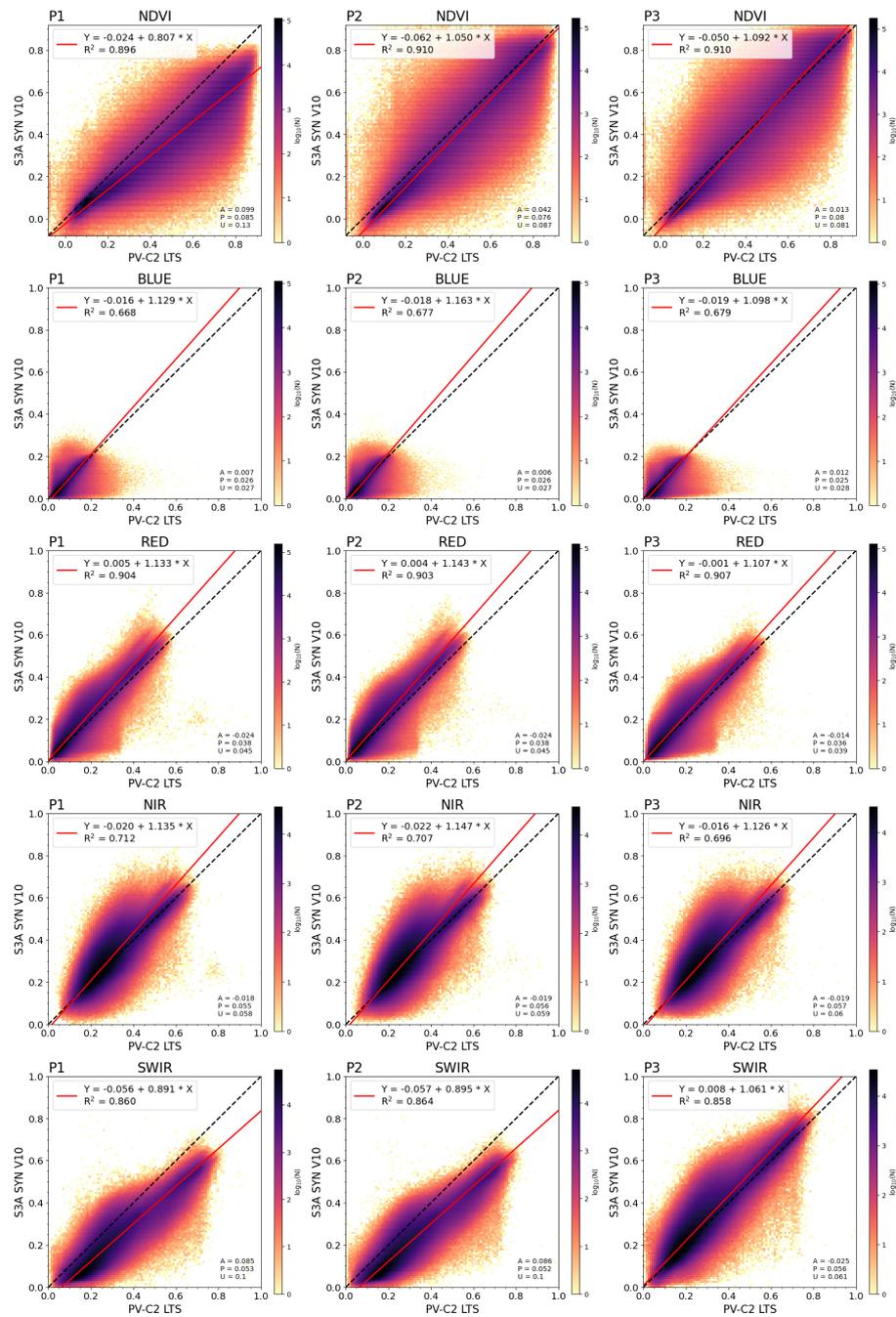
Figure 4. Scatter density plots and GM regression between PV-C2 LTS (X) and S3A SYN V10 (Y) for P1 (left), P2 (middle) and P3 (right). From top to bottom: NDVI, BLUE, RED, NIR and SWIR.
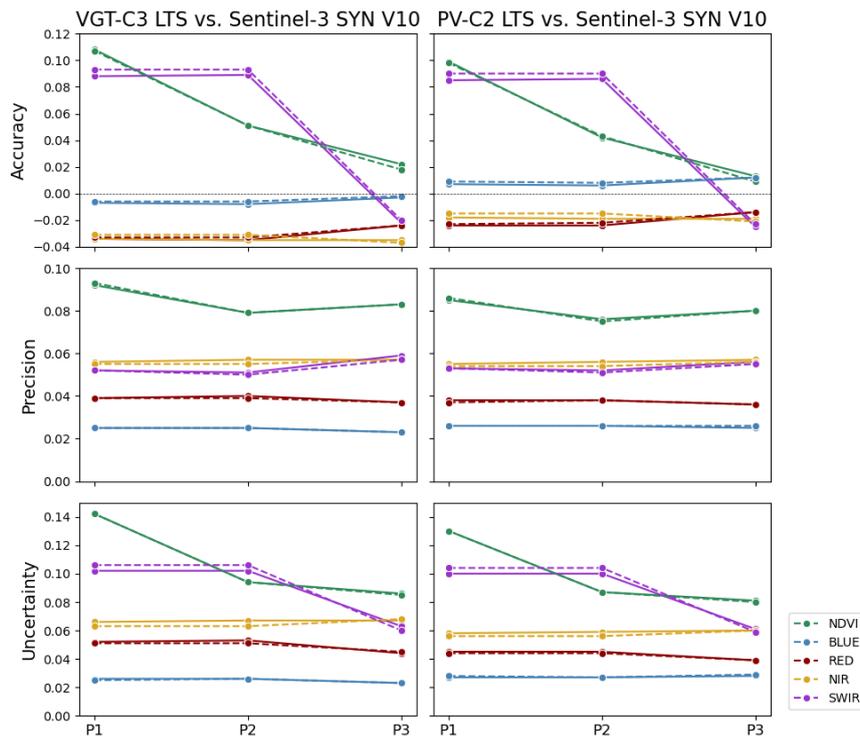
Figure 5. Evolution of *APU* metrics of the intercomparison of VGT-C3 LTS (left) and PV-C2 LST (right) and Sentinel-3A (solid lines) and Sentinel-3 (dashed lines) SYN V10 products from P1 to P3.

3.3. Current Consistency Level between Sentinel-3 SYN V10 Products and the SPOT VGT and PROBA-V Archives

Finally, Table 2 provides the *APU* metrics that are based on the latest 12 months of available Sentinel-3 SYN V10 data (P3), as these provide a measure of the current consistency level between SYN V10 and the SPOT VGT resp. PROBA-V archives. Overall, the consistency is higher with the PV-C2 LTS, with absolute *A* values around 0.01 (i.e. ±1% surface reflectance) for BLUE and RED, around -0.02 (-2%) for NIR and SWIR, and around 0.01 for the NDVI. Consistency with VGT-C3 is slightly higher for BLUE (*A* below 1%), similar for SWIR, and lower for RED and NIR (-2% and -4%, respectively) and the NDVI (0.02).

These consistency levels are in line with the initial expectations, based on simulated Medium Resolution Imaging Spectrometer (MERIS) and Advanced Along-Track Scanning Radiometer (AATSR) data, which stated that, depending on the spectral band, an accuracy of 3 to 5% could generally be expected [7].

Table 2. *APU* metrics for the intercomparison between the VGT-C3 and PV-C2 LTS and Sentinel-3 SYN V10 products for P3 (August 2023-July 2024). Statistics give a measure for the current consistency levels between Sentinel-3 SYN V10 and the SPOT VGT resp. PROBA-V product archives.

Intercomparison	Metric	BLUE	RED	NIR	SWIR	NDVI
VGT-C3 LTS vs. S3A SYN V10	A	-0.003	-0.024	-0.035	-0.022	0.022
	P	0.023	0.037	0.057	0.059	0.083
	U	0.023	0.044	0.067	0.063	0.086
VGT-C3 LTS vs. S3B SYN V10	A	-0.002	-0.024	-0.037	-0.020	0.018
	P	0.023	0.037	0.057	0.057	0.083
	U	0.023	0.045	0.068	0.060	0.085
PV-C2 LTS vs. S3A SYN V10	A	0.012	-0.014	-0.019	-0.025	0.013
	P	0.025	0.036	0.057	0.056	0.08
	U	0.028	0.039	0.06	0.061	0.081

PV-C2 LTS vs. S3B SYN V10	A	0.012	-0.014	-0.021	-0.023	0.009
	P	0.026	0.036	0.056	0.055	0.080
	U	0.029	0.039	0.06	0.059	0.080

4. Conclusions

Sentinel-3 SYN VGT products were designed to provide continuity to the SPOT VGT standard products, but since SPOT5 was decommissioned before the launch of the first Sentinel-3 satellite, PROBA-V acted as a gap filler, and thus consistency with PROBA-V is as (if not more) relevant. In principle, a continuous data series of standard TOA reflectance, daily and 10-day composite TOC reflectance and NDVI products should be available to users, for applications related to long-term, large-scale vegetation monitoring, climate change studies, agricultural monitoring, etc. However, some flaws were identified in the Sentinel-3 SYN VGT processing baselines, that were only gradually resolved in the course of the past years. These changes have progressively increased the quality of the Sentinel-3 SYN VGT products, as is evidenced through the spatio-temporal intercomparison of the combined time series of SPOT VGT, PROBA-V and Sentinel-3 SYN VGT 10-day NDVI composite products with an external reference from LSA-SAF, and the intercomparison of Sentinel-3 SYN V10 products with the LTS of VGT-C3 resp. PV-C2 for 3 distinct periods with different levels of product quality.

For the last 12 months of SYN V10 products, mean absolute bias values compared to the PV-C2 climatology of ~1% (for BLUE and RED surface reflectance), ~2% (for NIR and SWIR) and 0.01 (for NDVI) are reached. Consistency with VGT-C3 is slightly higher for BLUE, similar for SWIR, and slightly lower for RED and NIR and the NDVI. Overall, high dispersion of product retrievals around their expected values, i.e. high standard deviation of the bias, is observed, because of the many factors that influence the intercomparison.

The subsequent Sentinel-3 SYN VGT processing baseline updates have thus resulted in better quality products. Nevertheless, there are a few possible improvements that could still lead to better consistency with the SPOT VGT and PROBA-V product archives: (i) Enhancement of the atmospheric correction scheme, with more reliable AOT estimation; (ii) Improvements in the cloud and snow screening and inclusion of cloud shadow masking; (iii) Combination of S3A and S3B observations in single composite products to increase daily global coverage and to reduce the effect of residual cloud contamination; and (iv) Upgrade of the spatial resolution of SYN VGT products to 300 m (1°/336) to align with the higher resolution PROBA-V global data products archive.

Finally, from users' perspective, it is essential to reprocess the entire Sentinel-3 SYN VGT archive using the latest and most advanced processing baseline. The current archive is inconsistent, preventing users from accessing a uniform data set of standard SPOT VGT, PROBA-V and Sentinel-3 SYN VGT products. A consistent data record, spanning over 25 years from 1998 onwards, would provide valuable input for a wide range of applications.

Author Contributions: Conceptualization, CT and ES; Data curation, CT and CH; Formal analysis, CT; Methodology, CT and ES; Resources, CT, ES and CH; Software, CT and ES; Writing – original draft, CT; Writing – review & editing, CT, ES and CH.

Data Availability Statement: The original data presented in the study are openly available on the Copernicus Data Space Ecosystem at https://dataspace.copernicus.eu/ and on the Terrascope platform at https://terrascope.be/en.

Conflicts of Interest: The authors declare no conflicts of interest.

References

1. Henocq, C.; North, P.; Heckel, A.; Ferron, S.; Lamquin, N.; Dransfeld, S.; Bourg, L.; Toté, C.; Ramon, D. OLCI/SLSTR SYN L2 Algorithm and Products Overview. In Proceedings of the IGARSS 2018 - 2018 IEEE International Geoscience and Remote Sensing Symposium; IEEE, July 2018; Vol. 16, pp. 8723–8726.

12

2.   Donlon, C.; Berruti, B.; Buongiorno, A.; Ferreira, M.H.; Féménias, P.; Frerick, J.; Goryl, P.; Klein, U.; Laur, H.; Mavrocordatos, C.; et al. The Global Monitoring for Environment and Security (GMES) Sentinel-3 Mission. *Remote Sens Environ* **2012**, *120*, 37–57, doi:10.1016/j.rse.2011.07.024.

3.   Francois, M.; Santandrea, S.; Mellab, K.; Vrancken, D.; Versluys, J. The PROBA-V Mission: The Space Segment. *Int J Remote Sens* **2014**, *35*, 2548–2564, doi:10.1080/01431161.2014.883098.

4.   Dierckx, W.; Sterckx, S.; Benhadj, I.; Livens, S.; Duhoux, G.; Van Achteren, T.; Francois, M.; Mellab, K.; Saint, G. PROBA-V Mission for Global Vegetation Monitoring: Standard Products and Image Quality. *Int J Remote Sens* **2014**, *35*, 2589–2614, doi:10.1080/01431161.2014.883097.

5.   Toté, C.; Swinnen, E.; Sterckx, S.; Benhadj, I.; Dierckx, W.; Gomez-Chova, L.; Ramon, D.; Stelzer, K.; Van den Heuvel, L.; Clarijs, D.; et al. The Reprocessed Proba-V Collection 2: Product Validation. In Proceedings of the 2021 IEEE International Geoscience and Remote Sensing Symposium IGARSS; IEEE, July 11 2021; pp. 8084–8086.

6.   Toté, C.; Swinnen, E.; Van Den Heuvel, L.; Clarijs, D. *Evaluation of PROBA-V C2 Products Final Report*; https://proba-v.vgt.vito.be/sites/probavvgt/files/downloads/PROBA-V_C2_Evaluation.pdf; 2023.

7.   North, P.; Heckel, A. *SYN Algorithm Theoretical Basis Document*; https://earth.esa.int/documents/247904/349589/SYN_L2-3_ATBD.pdf, 2010.

8.   Clerc, S.; Donlon, C.; Borde, F.; Lamquin, N.; Hunt, S.E.; Smith, D.; McMillan, M.; Mittaz, J.; Woolliams, E.; Hammond, M.; et al. Benefits and Lessons Learned from the Sentinel-3 Tandem Phase. *Remote Sens (Basel)* **2020**, *12*, doi:10.3390/RS12172668.

9.   S3-MPC *Sentinel-3 SLSTR VIS and SWIR Channel Vicarious Calibration Adjustments*; https://sentinels.copernicus.eu/documents/247904/4620074/Sentinel-3-SLSTR-VIS-and-SWIR-Channel-Vicarious-Calibration-Adjustments.pdf/fef9161b-29d1-0578-0a7a-60246433a910; 2021.

10.   Toté, C.; Swinnen, E.; Sterckx, S.; Clarijs, D.; Quang, C.; Maes, R. Evaluation of the SPOT/VEGETATION Collection 3 Reprocessed Dataset: Surface Reflectances and NDVI. *Remote Sens Environ* **2017**, *201*, 219–233, doi:10.1016/j.rse.2017.09.010.

11.   Wolters, E.; Swinnen, E.; Toté, C.; Sterckx, S. *SPOT-VGT Collection 3 Products User Manual*; VITO, https://docs.terrascope.be/#/DataProducts/SPOT-VGT/ProductsOverview, 2016.

12.   Galvao, L.S.; Ponzoni, F.J.; Epiphanio, J.C.N.; Rudorff, B.F.T.; Formaggio, A.R. Sun and View Angle Effects on NDVI Determination of Land Cover Types in the Brazilian Amazon Region with Hyperspectral Data. *Int J Remote Sens* **2004**, *25*, 1861–1879, doi:10.1080/01431160310001598908.

13.   Sellers, P.J. Canopy Reflectance, Photosynthesis and Transpiration. *Int J Remote Sens* **1985**, *6*, 1335–1372, doi:10.1080/01431168508948283.

14.   Swinnen, E.; Verbeiren, S.; Deronde, B.; Henry, P. Assessment of the Impact of the Orbital Drift of SPOT-VGT1 by Comparison with SPOT-VGT2 Data. *Int J Remote Sens* **2014**, *35*, 2421–2439, doi:10.1080/01431161.2014.883100.

15.   Sterckx, S.; Benhadj, I.; Duhoux, G.; Livens, S.; Dierckx, W.; Goor, E.; Adriaensen, S.; Heyns, W.; Van Hoof, K.; Strackx, G.; et al. The PROBA-V Mission: Image Processing and Calibration. *Int J Remote Sens* **2014**, *35*, 2565–2588, doi:10.1080/01431161.2014.883094.

16.   Wolters, E.; Toté, C.; Dierckx, W.; M, P.; Swinnen, E. *PROBA-V Collection 2 Products User Manual*; https://proba-v.vgt.vito.be/sites/probavvgt/files/downloads/PROBA-V_C2_Products_User_Manual.pdf; 2023.

17.   Eerens, H.; Baruth, B.; Bydekerke, L.; Deronde, B.; Dries, J.; Goor, E.; Heyns, W.; Jacobs, T.; Ooms, B.; Piccard, I.; et al. Ten-Daily Global Composites of METOP-AVHRR. *Proc. of the 6th International Symposium on Digital Earth* **2009**, 8–13, doi:10.1117/12.873233.

18.   Duveiller, G.; Fasbender, D.; Meroni, M. Revisiting the Concept of a Symmetric Index of Agreement for Continuous Datasets. *Sci Rep* **2016**, *6*, doi:10.1038/srep19401.

19.   Vermote, E.F.; Kotchenova, S. Atmospheric Correction for the Monitoring of Land Surfaces. *Journal of Geophysical Research Atmospheres* **2008**, *113*, doi:10.1029/2007JD009662.

20.   Claverie, M.; Vermote, E.F.; Franch, B.; Masek, J.G. Evaluation of the Landsat-5 TM and Landsat-7 ETM+ Surface Reflectance Products. *Remote Sens Environ* **2015**, *169*, 390–403, doi:10.1016/j.rse.2015.08.030.

21.   Meroni, M.; Atzberger, C.; Vancutsem, C.; Gobron, N.; Baret, F.; Lacaze, R.; Eerens, H.; Leo, O. Evaluation of Agreement between Space Remote Sensing SPOT-VEGETATION FAPAR Time Series. *IEEE Transactions on Geoscience and Remote Sensing* **2013**, *51*, 1951–1962, doi:10.1109/TGRS.2012.2212447.

22.   Eklundh, L. Noise Estimation in NOAA AVHRR Maximum-Value Composite NDVI Images. *Int J Remote Sens* **1995**, *16*, 2955–2962.

23.   Niro, F. Evaluation of Orbital Drift Effect on Proba-v Surface Reflectances Time Series. *Remote Sens (Basel)* **2021**, *13*, doi:10.3390/rs13122250.

24.   Nagol, J.; Vermote, E.; Prince, S. Quantification of Impact of Orbital Drift on Inter-Annual Trends in AVHRR NDVI Data. *Remote Sens (Basel)* **2014**, *6*, 6680–6687, doi:10.3390/rs6076680.

25.   León-Tavares, J.; Roujean, J.L.; Smets, B.; Wolters, E.; Toté, C.; Swinnen, E. Correction of Directional Effects in Vegetation Ndvi Time-Series. *Remote Sens (Basel)* **2021**, *13*, doi:10.3390/rs13061130.

26. Holben, B.N. Characteristics of Maximum-Value Composite Images from Temporal AVHRR Data. *Int J Remote Sens* **1986**, *7*, 1417–1434.

27. Maisongrande, P.; Duchemin, B.; Dedieu, G. VEGETATION/SPOT: An Operational Mission for the Earth Monitoring; Presentation of New Standard Products. *Int J Remote Sens* **2004**, *25*, 9–14, doi:10.1080/0143116031000115265.

28. Gelaro, R.; McCarty, W.; Suárez, M.J.; Todling, R.; Molod, A.; Takacs, L.; Randles, C.A.; Darmenov, A.; Bosilovich, M.G.; Reichle, R.; et al. The Modern-Era Retrospective Analysis for Research and Applications, Version 2 (MERRA-2). *J Clim* **2017**, *30*, 5419–5454, doi:10.1175/JCLI-D-16-0758.1.

29. North, P.R.J.; Brockmann, C.; Preusker, R.; North, P.; Fischer, J.; Gomez-Chova, L.; Grey, W.; Heckel, A.; Moreno, J.; Preusker, R.; et al. MERIS/AATSR Synergy Algorithms for Cloud Screening, Aerosol Retrieval, and Atmospheric Correction. In Proceedings of the 2nd MERIS / (A)ATSR User Workshop; ESRIN, Frascati, 2008; pp. 22–26.

30. Wolters, E.; Toté, C.; Sterckx, S.; Adriaensen, S.; Henocq, C.; Bruniquel, J.; Scifoni, S.; Dransfeld, S. Icor Atmospheric Correction on Sentinel-3/OLCI over Land: Intercomparison with Aeronet, Radcalnet, and Syn Level-2. *Remote Sens (Basel)* **2021**, *13*, 1–26, doi:10.3390/rs13040654.